

# ChemComm

Accepted Manuscript



This is an *Accepted Manuscript*, which has been through the Royal Society of Chemistry peer review process and has been accepted for publication.

*Accepted Manuscripts* are published online shortly after acceptance, before technical editing, formatting and proof reading. Using this free service, authors can make their results available to the community, in citable form, before we publish the edited article. We will replace this *Accepted Manuscript* with the edited and formatted *Advance Article* as soon as it is available.

You can find more information about *Accepted Manuscripts* in the [Information for Authors](#).

Please note that technical editing may introduce minor changes to the text and/or graphics, which may alter content. The journal's standard [Terms & Conditions](#) and the [Ethical guidelines](#) still apply. In no event shall the Royal Society of Chemistry be held responsible for any errors or omissions in this *Accepted Manuscript* or any consequences arising from the use of any information it contains.

## COMMUNICATION

Cite this: DOI:  
10.1039/x0xx00000x

# A Robust and Conductive Metal-Impregnated Graphene Oxide Membrane Selectively Separating Organic Vapors

Do Van Lam,<sup>a, b, †</sup> Tao Gong,<sup>c, †</sup> Sejeong Won,<sup>d</sup> Jae-Hyun Kim,<sup>b</sup> Hak-Joo Lee,<sup>b</sup> Changgu Lee,<sup>c, e</sup> and Seung-Mo Lee<sup>a, b, \*</sup>

Received 00th January 2012,  
Accepted 00th January 2012

DOI: 10.1039/x0xx00000x

www.rsc.org/

**Tiny amount of Zn impregnated by ALD triggered mechanical as well as electrical properties enhancement in the graphene oxide (GO) membrane. In addition, the Zn-impregnated membranes selectively separated diverse organic vapors while maintaining high water permeability.**

Graphene oxide (GO) membrane has been lately emerged as one of the most researched nanomaterials.<sup>1</sup> It has been conveniently synthesized from graphite flakes consisting of monolayer to several layers of graphene sheet and features oxygenated functionalities on basal planes and along sheet edges.<sup>2</sup> These sheets can be easily reassembled into well-stacked structures of free-standing, large-area membranes through vacuum-assisted assembly<sup>3</sup> of GO dispersions. The stacked GO membrane has continuously come into spotlight as an innovative material for gas separation on the strength of recent several scientific breakthroughs.<sup>4</sup> The unique permeation properties of the membrane make it useful for certain applications. However, unfortunately, the as-made GO is electrically insulating, which largely interferes with technological progress. Although reduction of GO improves their electrical conductivities,<sup>5</sup> the reduction causes removal of the functional groups and shrinkage of the intersheet spacing, thereby leading to closing of GO nanocapillaries and consequently stopping the permeation of all gases and liquids.<sup>6</sup> To make matters worse, the membrane becomes extremely fragile and contains many structural defects after conventional reduction.<sup>6</sup> Here we report that atomic layer deposition (ALD) can be a one-pot post-processing method to prepare not only mechanically robust but also electrically conductive GO membrane capable of selectively separating organic vapors and concurrently maintaining high water permeability.

ALD is basically based on surface chemistry of substrate materials employed, which has been generally regarded as one of thin film deposition techniques. However, ALD film growth on certain carbon-based materials with structural defects or hydrogen bonds was quite different from the growth on other materials. The unique ALD chemistry related to film nucleation and growth enabled structural defects existing in CVD-graphene to be selectively healed.<sup>7</sup> The self-limited growth nature of ALD (particularly, water-based metal oxides ALD) allowed various transition metal elements to be infiltrated into materials with hydrogen bonds.<sup>8</sup> GO is oxidized

graphene sheets with numerous oxygenated functional groups like epoxide and hydroxyl groups on basal planes, carbonyl and carboxyl groups along sheet edges.<sup>9</sup> In the metal oxide ALD using H<sub>2</sub>O as an oxygen source, H<sub>2</sub>O vapor is adsorbed on the substrate, forming a

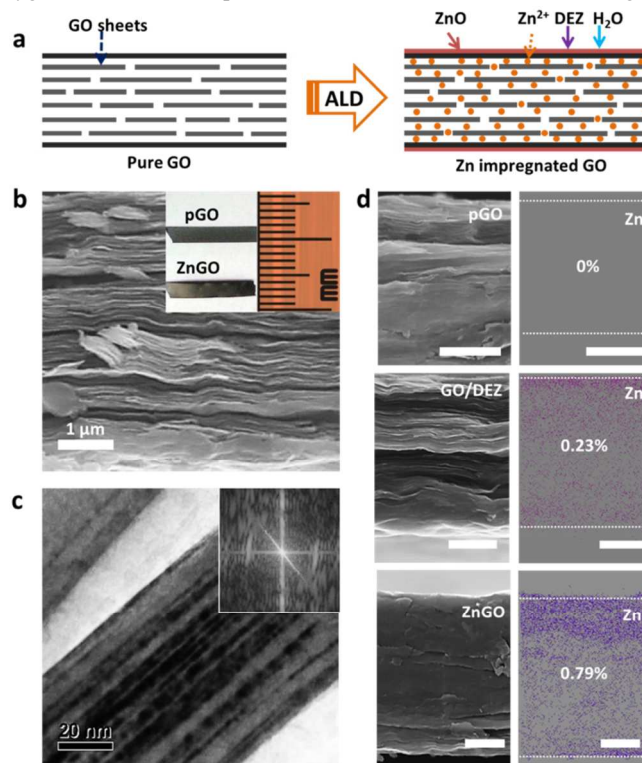


**Figure 1.** (a) Schematics of ZnGO membranes. (b) SEM (scanning electron microscope) cross section image of a pure GO showing its well-stacked structures and digital image inset of pGO & ZnGO. (c) TEM (transmission electron microscope) cross-section image of a GO piece and its corresponding FFT (fast Fourier transform) image. (d) The left panels were SEM cross-section images of pGO, GO/DEZ, and ZnGO, respectively; the right panels were the corresponding EDX mapping images of Zn element. Scale bar is 2  $\mu$ m.

hydroxyl group. Then, metal source reacts with the adsorbed hydroxyl groups. Considering ALD film formation mechanism and molecular structure of the GO, it is readily predictable that metal element of ALD reactant is likely impregnated into the interlayers of the GO membrane, thereby bridging GO interlayers through covalent bonds of GO oxygenated functionalities with metal ions (Figure 1a), although the properties of the resulting metal-impregnated GO remain to be looked into.

In this study, GO sheets were prepared using modified Hummers' method<sup>10</sup> to yield aqueous dispersions, followed by vacuum-assisted filtration to fabricate GO membranes. On the as-prepared GO membranes (pGO) having well-stacked layered structures (Figure 1b and 1c), 50 cycles of ZnO-ALD (growth rate of  $\sim 2.0$  Å/cycle) using diethylzinc (DEZ) and H<sub>2</sub>O as precursors was carried out at 70 °C (ZnGO). Exposure and purge time were adjusted to be long enough so that a full adsorption and impregnation of DEZ vapors into micrometer-thick GO membranes was able to be achieved. In consideration of the fact that the pGO has plentiful oxygenated groups (like, -OH) which can directly react with DEZ vapors, some GO membranes were treated with DEZ precursor only (GO/DEZ), and other membranes were simply annealed under the same processing temperature (70 °C) and time as ZnO-ALD process (pGO/A). Then, EDX (energy dispersive X-ray spectroscopy) mappings of Zn element for the prepared different GO membranes were performed to verify whether Zn impregnation into GO really occurs. As can be seen in Figure 1d, while no Zn was detected in pGO, Zn contents in ZnGO were  $\sim 0.79$  %, which was  $\sim 3$  times higher than that in GO/DEZ upon the same number of ALD cycles. These observations indicated that Zn can be controllably impregnated into the GO interlayers, and oxygenated groups existing on the GO surface can be also reacted with DEZ. Similar cases were also observed in Ti-impregnated GO and Hf-impregnated GO (Figure S1). It clearly demonstrated the broad applicability of ALD tool to our approach.

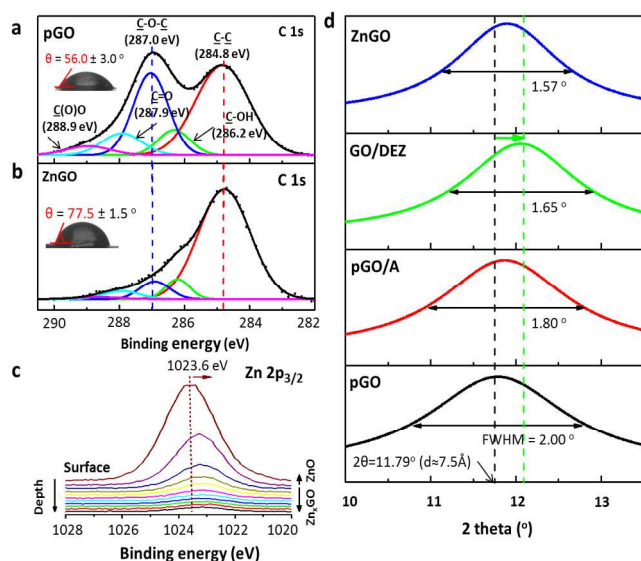


**Figure 2.** (a-b) Deconvoluted C 1s orbital XPS spectra of pGO and ZnGO, respectively. The insets were the corresponding water contact angles ( $\theta$ ) of the specimens. (c) XPS spectra of Zn 2p<sub>3/2</sub> orbital by depth for ZnGO. (d) XRD spectra of diverse GO membranes.

The chemical compositions and binding states of GO before and after Zn impregnation by ALD were characterized by X-ray photoelectron spectroscopy (XPS). The deconvoluted C 1s spectrum

of pGO (Figure 2a) showed peaks at 284.8, 286.2, 270.0, 287.9, and 288.9 eV, which are corresponding to the C in graphite, C-OH, C in epoxide, C=O, and O-C=O.<sup>8</sup> Figure 2b shows the typical C 1s spectrum inside ZnGO after etching the surface ZnO layer by Ar sputtering. Notably, the strong carbon epoxide peak intensity decreased upon Zn infiltration. This was likely originated from epoxide ring-opening reaction to form C-OH groups by H<sub>2</sub>O and Lewis acidic Zn ions.<sup>11</sup> The increase in water contact angle ( $\theta$ ) of ZnGO membranes indicated a large change in their surface chemistry. The downshifts in binding energies in XPS depth profile of Zn 2p<sub>3/2</sub> suggest the formation of covalent bonds between Zn and other elements inside ZnGO (Figure 2c). The atomic percentage of C, O, and Zn by depth showed the nearly uniform distribution of Zn likely in the Zn-impregnated region (Figure S2), which was consistent with the EDX mapping results in Figure 1d. It is also noted that the surface roughness of the ZnGO membranes was almost similar to the pGO membranes, while the surface friction force was nearly double, indicating negligible change of surface topology and successful integration of ZnO surface layer (Figure S3).

Because the spacing between GO layers is a crucial factor to determine gas separation and mechanical properties of the prepared GO membrane, X-ray diffraction (XRD) study was performed to evaluate the changes of the intersheet distance after ALD treatment. The intersheet spacing (*d*-spacing) of the pGO was measured to be  $\sim 7.5$  Å and observed to be further reduced after thermal annealing and Zn-impregnation (Figure 2d). GO/DEZ showed the smallest *d*-spacing presumably due to the highest loss of H<sub>2</sub>O through evaporation and reaction with DEZ. ZnGO had similar *d*-spacing to pGO/A, which can be explained by effect of intercalated Zn. Considering the bond lengths of 1.43 Å for C-O and 1.97 Å for Zn-O,<sup>12</sup> it would require at least two Zn ions to bridge two adjacent sheets with spacing of  $\sim 7.44$  Å (Figure 3). In addition, ZnGO exhibits the sharpest peak, indicating that the ZnGO has the highest degree of graphitization and the structural defects initially existing in the pGO are by and large healed by the impregnated Zn.<sup>13</sup> Moreover, the high blueshift in D bands of Raman spectra (Figure S4) probably indicates the heavier vibration of C-C bond at defective sites of GO sheets or the formation of new bonds at oxygenated functionalities, while the stability in G bands refers to the intactness of C-C bond at pristine areas.

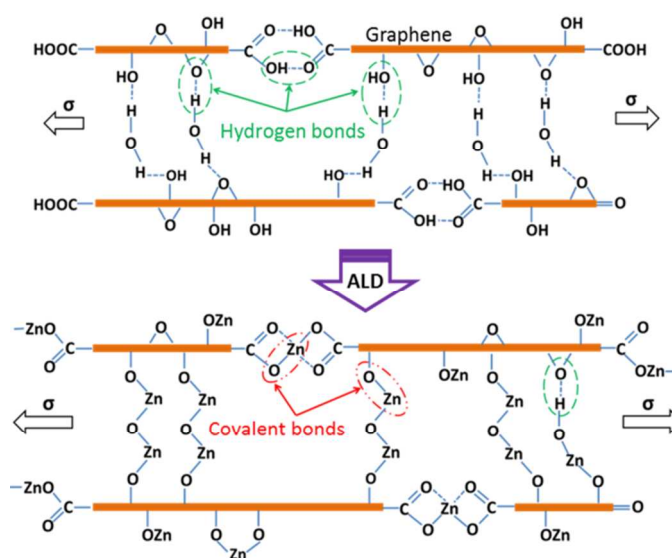


**Figure 3.** Presumable molecular structure changes of GO after Zn-impregnation.

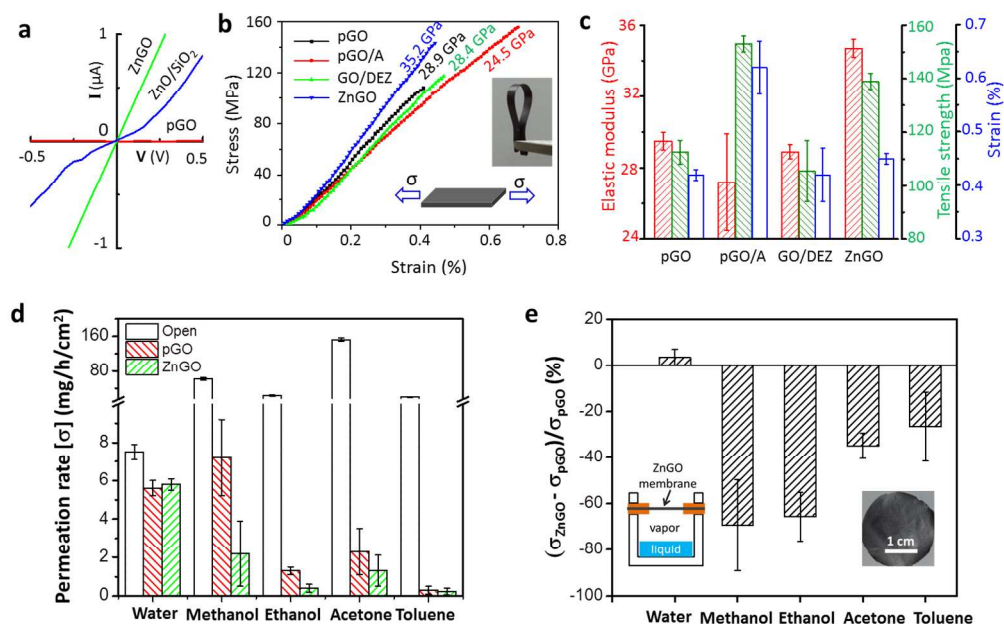


**Figure 4.** (a) IV characteristics of GO strips before and after ZnO-ALD. (b) Representative tensile testing curves of various GO strips. (c) Summary of mechanical properties for these specimens. (d) Permeation rates for different organic vapors through an open 1-cm<sup>2</sup> aperture container sealed with pGO and ZnGO membranes. (e) Permeation rate difference ratios of these vapors through the membranes. The positive ratio of water indicates enhancement in water permeation while negative ratios of other organic vapors refer to enhancements in blocking capability of the ZnGO membranes. The inset is schematics of experimental apparatus.

The changes in the physical and chemical properties of the GO caused by Zn-impregnation were found to be dramatic. While the pure GO were electrically nonconductive with average conductivity of  $\sim 10^{-3} \text{ S.m}^{-1}$ , the Zn impregnated GO showed the surface resistance of  $\sim 250 \text{ k}\Omega/\text{sq}$  and bulk conductivity of  $\sim 1 \text{ S.m}^{-1}$ , which is 3-order higher than that of the pure GO (Figure 4a). More importantly, the ZnGO showed to an appreciable extent higher conductance than ZnO film deposited on SiO<sub>2</sub> wafer at the same conditions as the ZnGO. This could be explained by the effect of the few-nanometer thin conductive ZnO layer deposited on the pure GO surface and the impregnated Zn atoms covalently bridging GO interlayers. In addition, the abundance of oxygenated functionalities in GO compared to Si presumably led to superior conductance of the ZnGO to the ZnO/SiO<sub>2</sub>.

The change of the mechanical properties was even more noteworthy. The typical stress-strain curves for various GO membranes were shown in Figure 4b. Since mechanical properties of GO membranes might be thickness-variant, we eliminated variations in thicknesses by using nearly identical GO strip specimens prepared from a single membrane with uniform thickness. The pGO strips of 7  $\mu\text{m}$  thick have average stiffness and tensile strength of  $\sim 29.5 \text{ GPa}$  and  $\sim 112 \text{ MPa}$ , respectively (Figure 4c). The annealed GO exhibited increased tensile strength and strain, but slightly decreased stiffness, while the GO/DEZ was observed to be nearly unchanged mechanical properties. In the case of ZnGO, the stiffness and tensile strength were noticeably  $\sim 20 \%$  and  $27 \%$  higher than those of the pGO strips, respectively. It is foreseeable that the pure GO resists to tensile loading by the long-range hydrogen bonds within intersheet galleries and edge-bound interactions. Provided that the hydrogen bondings ( $-\text{COOH}$  groups on two adjacent GO sheets and  $-\text{OH}$  groups on basal planes) in GO are replaced with metal-mediated covalent bonds (Figure 3), most likely the resulting GO shows remarkably enhanced stiffness and tensile strength in some way analogous to the enhancements by  $\text{Ca}^{2+}$  and  $\text{Mg}^{2+}$  ions.<sup>11</sup>

In order to demonstrate gas separation properties of the ZnGO membranes, vapor phase permeation tests were carried out at room conditions. Figure 4d and 4e summarize the permeation rates through the aperture with/without the membranes for various organic vapors. Although the evaporation rates of the organic molecules were much higher than that of water (water: methanol: ethanol: acetone: toluene = 1: 8.2: 3.1: 20.1: 2.6), their permeation rates through the pGO membranes were much lower than their evaporation rates. Interestingly, the water permeation rate through the ZnGO membranes was comparable to the pGO membranes while the permeation rates of other vapors were sharply reduced by  $\sim 70 \%$ ,  $65 \%$ ,  $35 \%$ , and  $26 \%$  for methanol, ethanol, acetone, and toluene, respectively (Figure 4e). The intersheet spacing of the GO membranes and structural defects in the GO are major pathways occurring molecular transports. Because the ZnO-ALD was found to heal defects within carbonous materials<sup>7</sup> and cause the reduction of intersheet spacing (Figure 2d), we initially anticipated highly limited transport behaviors of all vapors employed through ZnGO membrane. However, the results were out of our expectation. It appears that the hydrogen bonds and polarity determine the separation properties of the ZnGO. Namely, the presence of hydrogen bonds in GO results in the slower diffusion of water.<sup>6</sup> In ZnGO, as already demonstrated above, the impregnated Zn destroys hydrogen bonds and active groups within intersheet galleries, which likely facilitate the movement of water. Furthermore, since the penetration of organic molecules through GO membranes depends on both molecular size and their polarity,<sup>14</sup> the presence of Zn inside the intersheet galleries presumably generates larger energy barriers, which prevent organic molecules of larger size and lower polarity from penetrating into the ZnGO membranes (Table S1). Besides, our membranes also showed comparative results for separation efficiency to other GO based membranes from literature (Table S2).

In conclusion, through the vapor phase metal-impregnation effect observed in the conventional ZnO-ALD process, the properties of the GO were able to be easily modulated. Tiny amounts of Zn

impregnated by ALD triggered mechanical as well as electrical properties enhancement in the GO membrane. More importantly, the membranes selectively separated diverse organic vapors while unimpededly permeating water. Our ALD based method could be a surprisingly simple and extremely useful mean to tailor the properties of the GO membranes as well as other nanoporous materials commonly used for separation and purification technology.

This research was supported by the R&D Convergence Program of MSIP (Ministry of Science, ICT and Future Planning) and NST (National Research Council of Science & Technology) of Republic Korea (Grant CAP-13-2-ETRI), and the internal research program of Korea Institute of Machinery and Materials (SC1020).

## Notes and references

<sup>a</sup> Nano Mechatronics, Korea University of Science and Technology (UST), 217 Gajeong-ro, Yuseong-gu, Daejeon 305-333, South Korea.

<sup>b</sup> Department of Nanomechanics, Korea Institute of Machinery and Materials (KIMM), 156 Gajeongbuk-ro, Yuseong-gu, Daejeon 305-343, South Korea.

<sup>c</sup> SKKU Advanced Institute of Nano Technology (SAINT), Sungkyunkwan University, 2066 Seobu-ro, Suwon 440-746, South Korea.

<sup>d</sup> Department of Mechanical Engineering, Korea Advanced Institute of Science & Technology (KAIST), 291 Daehak-ro, Yuseong-gu, Daejeon 305-701, South Korea.

<sup>e</sup> School of Mechanical Engineering, Sungkyunkwan University, Seobu-ro, Suwon 440-746, South Korea.

<sup>†</sup> These authors equally contribute to this work.

\* Corresponding authors: <sup>a, b</sup> sm.lee@kimm.re.kr

Electronic Supplementary Information (ESI) available: detailed experimental procedure, supporting figures. See DOI: 10.1039/c000000x/

- 1 (a) C. N. R. Rao, A. K. Sood, K. S. Subrahmanyam, A. Govindaraj, *Angew. Chem. Int. Ed.* 2009, **48**, 7752–7777; (b) O. C. Compton, S. T. Nguyen, *Small* 2010, **6**, 711–723.
- 2 D. R. Dreyer, S. Park, C. W. Bielawski, R. S. Ruoff, *Chem. Soc. Rev.* 2010, **39**, 228–240.
- 3 (a) D. A. Dikin, S. Stankovich, E. J. Zimney, R. D. Piner, G. H. Dommett, G. Evmenenko, S. T. Nguyen, R. S. Ruoff, *Nature* 2007, **448**, 457–460; (b) H. Chen, M. Müller, K. Gilmore, G. Wallace, D. Li, *Adv. Mater.* 2008, **20**, 3557–3561.
- 4 (a) H. Huang, Y. Ying, X. Peng, *J. Mater. Chem.* 2014, **2**, 13772–13782; (b) H. W. Kim, H. W. Yoon, S. M. Yoon, B. M. Yoo, B. K. Ahn, Y. H. Cho, H. J. Shin, H. Yang, U. Paik, S. Kwon, J. Y. Choi, H. B. Park, *Science* 2013, **342**, 91–95; (c) H. W. Kim, H. W. Yoon, B. M. Yoo, J. S. Park, K. L. Gleason, B. D. Freeman, H. B. Park, *Chem. Commun.* 2014, **50**, 13563–13566.
- 5 (a) X. Cao, D. Qi, S. Yin, J. Bu, F. Li, C. F. Goh, S. Zhang, X. Chen, *Adv. Mater.* 2013, **25**, 2975–2962; (b) U. N. Maiti, J. Lim, K. E. Lee, W. J. Lee, S. O. Kim, *Adv. Mater.* 2014, **26**, 615–619; (c) C. Wang, D. Li, C. O. Too, G. G. Wallace, *Chem. Mater.* 2009, **21**, 2604–2606.
- 6 R. R. Nair, H. A. Wu, P. N. Jayaram, I. V. Grigorieva, A. K. Geim, *Science* 2012, **335**, 442–444.
- 7 D. V. Lam, S. M. Kim, Y. Cho, J. H. Kim, H. J. Lee, J. M. Yang, S. M. Lee, *Nanoscale* 2014, **6**, 5639–5644.

- 8 (a) S. M. Lee, V. Ischenko, E. Pippel, A. Masic, O. Moutanabbir, P. Fratzl, M. Knez, *Adv. Funct. Mater.* 2011, **21**, 3047–3055; (b) S. M. Lee, E. Pippel, U. Gösele, C. Dresbach, Y. Qin, C. Chandran, T. Bräuniger, G. Hause, M. Knez, *Science* 2009, **324**, 488–492.
- 9 (a) H. He, J. Klinowski, M. Forster, A. Lerf, *Chem. Phys. Lett.* 1998, **287**, 53–56; (b) A. Lerf, H. He, M. Forster, J. Klinowski, *J. Phys. Chem. B* 1998, **102**, 4477–4482.
- 10 W. S. Hummers, R. E. Offeman, *J. Am. Chem. Soc.* 1958, **80**, 1339–1339.
- 11 S. Park, K. S. Lee, G. Bozoklu, W. Cai, S. T. Nguyen, R. S. Ruoff, *ACS Nano* 2008, **2**, 572–578.
- 12 A. Nimmermark, L. Öhrström, J. Reedijk, *Z. Kristallogr.* 2013, **228**, 311–317.
- 13 S. Pei, H. M. Cheng, *Carbon* 2012, **50**, 3210–3228.
- 14 R. Liu, G. Arabale, J. Kim, K. Sun, Y. Lee, C. Ryu, C. Lee, *Carbon* 2014, **77**, 933–938.